IJME

Int. J. of Applied Mechanics and Engineering, 2025, vol.30, No.3, pp.57-74
DOI: 10.59441/ijame/203786

FLOW AND HEAT TRANSFER OF HYBRID JEFFREY NANOFLUID NEAR A RIGA PLATE WITH NON-LINEAR CONVECTION

T. Fayaz[1], M.S. Ansari[1*], O. Otegbeye[2] and M. Trivedi[3]
[1]Department of Mathematics, Pandit Deendayal Energy University, INDIA
[2]School of Computer Science and Applied Mathematics, Faculty of Science,
University of the Witwatersrand., SOUTH AFRICA
[3]Institute of Management, Nirma University, INDIA
E-mail: shariffuddin@gmail.com

Hybrid nanofluid, an extension of nanofluid, is the hybridization of dissimilar type of nanoparticles dispersed into the base fluid. Engineers, manufacturers and developers are fascinated to imply hybrid nanofluid in various applications such as, biomedical, electronic generators, heat pipes, refrigerations, transformer cooling and heat exchangers due to its unique speciality in terms of thermophysical properties, heat transfer performance and stability. The present study deals on heat transfer in an unsteady magnetohydrodynamic hybrid nanoliquid composed of (i) silver and gold and (ii) aluminium oxide and copper oxide nanoparticles considering base fluid as ethylyne glycol, flow over a Riga plate. The impact of viscous dissipation, non-linear convection, magnetic field and convective boundary condition are also integrated in this study. The nonlinear and coupled partial differential equations, which describe the flow system, are nondimensionalized keeping in same form. Solution of nondimensionalized PDEs is reaped by exercising spectral quasilinearization method. The substantiation of convergence and accuracy is also presented. Obtained solutions are presented in terms of graphs and tables to survey the flow and temperature behaviours. It is found that fluid velocity is smaller in the hybrid nanofluid containing silver and gold nanoparticles whereas an improved heat transfer rate is seen for hybrid nanoliquid containing aluminium oxide and copper oxide nanoparticles. This study may be helpful in various scientific and industrial applications concerning boundary layer separation and heat transfer.

Key words: Jeffrey hybrid nanofluid, Riga plate, non-linear convection, convective conditions, spectral quasi-linearization method

1. Introduction

Nanofluid plays a highly significant role in contemporary research and has several uses in the processing of phenomena related to heat distribution. When compared to conventional fluids, systems using nanofluid as a working fluid can offer superior heat dispersion and thermal performance. Following the promising experiment by Choi *et al.* [1], the concept of nanofluid finds widespread use in engineering and biological research, as well as in all branches of nanotechnology. Alrabaiah *et al.* [2] examined the properties of nanofluids and their applications, focussing on different nanoparticles in base fluids. A statistical analysis of experimental based mathematical models for thermal conductivity of nanofluid, establishing a correlation to predict thermal conductivity, was carried out by Molana *et al.* [3]. A conceptual analysis on obstacles to the nanofluid mechanism and their cutting-edge applications in contemporary science and commerce was presented by Alagumalai *et al.* [4]. Arif *et al.* [5] studied a flow of nanofluid with discontinuous boundary temperature employing molybdenum disulphide and graphene nanoparticles in engine oil. Ali *et al.* [6] investigated the heat transfer characteristics of nanofluid combining molybdenum disulphide nanoparticles in polyethylene glycol base fluid, integrating the impact of radiation, porosity and chemical reaction near a vertical plate. Iqbal *et al.* [7] analysed heat transmission in buoyancy driven nanoliquid flow at a stretchable surface considering Joule heating and constant/prescribed wall temperature. Senthilvadivu *et al.* [8] considered

* To whom correspondence should be addressed

radiation and viscous dissipation on heat transfer analysis of Darcy-Forchheimer flow of Casson nanofluid containing single walled and multi-walled carbon nanotubes at a Riga plate. Ganga *et al.* [9] explored the behaviour of axisymmetric nanofluid flow over a nonlinearly stretched sheet influenced by a magnetic field by taking into account factors like Brownian motion, thermophoresis, as well as the Dufour and Soret effects. Mesbah *et al.* [10] assessed entropy in free convection MHD flow of a micropolar nanofluid over a vertical, moving, and permeable plate by considering the effects of viscous dissipation. Medisetty *et al.* [11] analysed the oscillatory MHD flow in a horizontal porous channel containing two immiscible nanofluids by considering factors like velocity and thermal slip, thermal radiation, Joule heating, and dissipation effects. The research uses aluminium oxide (Al_2O_3) and copper (Cu) nanoparticles suspended in water as the base fluid and employs the Maxwell-Garnett model to assess thermal conductivity. Samad Khan *et al.* [12] elaborated hybrid nanofluid flow near a Riga plate embedded in a variable porous space. Single- and multi-walled carbon nanotubes and water are used to prepare the considered hybrid nanofluids. Bilal *et al*. [13] scrutinised effects of thermophoresis, variable thermal conductivity, and Brownian diffusion on flow and heat transfer of unsteady Micropolar nanofluid stretched flow across a vertically oriented magnetized surface.

A hybrid nanofluid is described as the dispersion of two or more different nanocomposites in a single base fluid. Numerous practical scenarios involving hybrid nanofluid revealed excellent thermal conductivity. However, a sophisticated cooling technique with outstanding thermal performance is still necessary in the fields of thermal and modern science. Because of this, scientists have found that hybrid nanoliquid performance is superior to that of ordinary fluids/nanofluids. In order to achieve high thermal efficiency in various systems, hybrid nanofluid is now a better option for scientists/ researchers. A brief literature survey concerning flow and heat transfer of hybrid nanofluid under different conditions and configurations are summarised in Tab.1.

Table 1. Studies involving hybrid nanofluids in various geometries.

Authors	Base fluid	Nanoparticles	Geometry and effects
Tlili *et al.* [14]	Methanol	Aluminium alloys AA7072, AA7075	stretched plane of variable thickness, slip effects
El-Zahar *et al.* [15]	Water	Alumina and Copper	horizontal circular cylinder, convective boundary conditions, non-linear radiation phenomenon
Alarabi *et al.* [16]	Water	Alumina and Copper	stretching and shrinking cylinder, heterogeneous–homogeneous chemical reactions, magnetic field and joule heating
Mahdy *et al.* [17]	Water	Alumina and Copper	vertical rotating permeable plate in a porous medium, internal heat generation, magnetic field and thermal radiation.
El-Zahar *et al.* [18]	Water	Silver and Titanium	impulsively rotating sphere, mixed convection, magnetic field, stagnation point flow.
Hossam *et al* [19]	Sodium Alginate	Silver and Sodium Alginate	non-isothermal wedge in a porous medium, radiation, velocity slip and mixed convection
Zhang *et al.* [20]	Kerosene	Tantalum and Nickel	porous elastic surface, viscous dissipation and induced magnetic field effect
Lone *et al.* [21]	Water	Alumina and silver	vertical flat surface, effects of suction and injection, mixed convection, viscous dissipation, thermal radiation, and joule heating were incorporated
Rekha *et al.* [22]	Water	Aluminium alloys AA7072 and AA7075	cone, wedge, and plate

Table 1 cont. Studies involving hybrid nanofluids in various geometries.

Authors	Base fluid	Nanoparticles	Geometry and effects
Verma *et al.* [23]	Pure water	Copper and Aluminium Oxide	between two rigid non-parallel plane walls
Jaafar *et al.* [24]	Water	Copper and Aluminium Oxide	nonlinearly stretching and shrinking surface
Ullah *et al.* [25]	Water	Copper and Alumina	stretching surface in porous medium
Rao and Deka [26]	Water	Silver (Ag) and Alumina (Al_2O_3)	stretching sheet of porous medium
Verma and Meher [27]	Water	Copper and Gold	non-parallel plate embedded in permeable stretchable convergent and divergent channels
Imoro *et al.* [28]	Blood	Gold and Copper	stenosed artery, viscous dissipation, joule heating, and stenosis-induced height effects
Naik *et al.* [29]	Water	Titanium dioxide, Cobalt ferrite, and Magnesium oxide	bidirectional stretching sheet, effects considered are viscous dissipation, cattaneo–christov heat flux, ohmic heating, thermal radiation, and irreversibility
Tao *et al.* [30]	Water	Carbon nanotubes and Graphene nanoplatelets	cylindrical pipe as geometry with inlet, outlet, convective, and no-slip boundary condition
Maiti *et al.* [31]	Water	Copper and Aluminium oxide $(Cu-Al_2O_3))$	stagnation point flow over a stretching disk

Riga plate refers to a sophisticated magnetic field mechanism that may be created by adjusting a group of permanent magnets and alternative electrodes over a plane surface. This plate has the ability to create a streamwise Lorentz force in weakly conducting fluids, which can control the structures of boundary layer separation, turbulence and skin friction. It is well known that a control over EMHD fluid flow can be achieved by using electric field and magnetic fields. Riga plate is the one that is helpful in this regard. The Riga plates are highly advantageous and useful in various fluid flows particularly in submarines, which assists to lowering skin friction. Considering these, a number of research articles dealing hybrid nanofluid over an electromagnetic surface are available in literature. Of which, Ansari *et al.* [32] reported the flow process of Jeffrey nanofluid flow on a Riga surface, incorporating the effects of viscous dissipation, uneven heat source/sink, Brownian motion, and thermophoretic force. Prabakaran *et al.* [33] elaborated an unsteady Darcy Forchheimer flow of hybrid nanofluid (composed of water and kerosene as base fluid and single and multiwall carbon nanotubes as nanoparticles) over a Riga plate. Wahid *et al.* [34] analysed a velocity slip on hybrid nanofluid stagnation point flow at shrinking Riga plate. Considered hybrid nanofluid comprises of magnetite - cobalt ferrite nanoparticles and water as base fluid. Ali *et al.* [35] reported a work focussing on the flow of hybrid nanofluid, (Al_2O_3-Cu)/ water, over a Riga plate. This work is accompanied by many influential factors like thermal radiation, entropy generation, viscous dissipation, heat flux, convective boundary conditionsand slippage. Algehyne *et al.* [36] considered a three-dimensional stretchable flow of hybrid nanofluid (water, molybdenum disulphide (MoS_2) and magnesium oxide (MgO) nanoparticles) at a Riga plate with chemical reaction effects. Yasmin *et al.* [37] obtained a homotopic solution of hybrid nanofluid (water/copper-aluminium) on a bi-directional Riga plate deliberating Cattaneo-Christov model for heat and mass flux. Siddique *et al.* [38] reported an analysis on heat transfer of hybrid nanofluid (engine oil as base fluid and copper-aluminium nanoparticles) stretching/shrinking flow over a Riga wedge by employing fuzzification of nanoparticle volume fraction. Khan *et al.* [39] debated a drug delivery application via Casson hybrid nanofluid (blood as a base

fluid and single and multi-walled carbon nanotubes as nanoparticles) at a riga plate. It reveals an improved heat transfer characteristics of Casson hybrid nanofluid on Riga surface which is helpful in local drug delivery applications. Upreti *et al.* [40] presented a comparative study on Darcy-Forchheimer flow of Casson fluid, Casson nanofluid and Casson hybrid nanofluid over porous Riga plate. Hybrid nanofluid exhibits an improved flow characteristics than nanofluid and pure fluid.

Comprehensive review on existing literature leads to conclusion that the study on flow and heat transfer of hybrid nanofluid near a Riga plate in combination of magnetic field with non-linear convection is rare. Hence, authors attempt to perform this novel study. This study may find applications in controlling the boundary layer separation, turbulence and skin friction, biomedical, electronic generators, heat pipes, refrigerations, transformer cooling and heat exchangers. The distinctiveness of this study lies in the meticulous consideration of nonlinear convection in time-dependent flow of hybrid nanofluids, specifically $(Ag-Au)$ /Ethylene glycol and (Al_2O_3-CuO)/Ethylene glycol, over a convectively heated Riga surface. To the best of our knowledge, no study has been carried out for the flow of hybrid nanofluids past a Riga surface under considered conditions. By employing a set of transformations, the governing partial differential equations of the proposed model are nondimensionalized. These equations are solved numerically using an efficient numerical method, namely Spectral Quasilinearization Method (SQLM). The results are presented through a variety of plots and numerically constructed tables and discussed the flow and heat transfer aspects in detail. The structure of present analysis is as follows: a detailed mathematical formulation, outline of solution methodology, convergence and accuracy of solution method, results analysis, and summary of work. Following are the points that describe the novelty and newness of this study:

- This is concerned to flow of a hybrid Jeffrey nanofluid near an impulsive moving convectively heated Riga plate in combination of magnetic field.
- Two hybrid nanofluids, composed of (i) silver and gold (*Ag-Au*) and (ii) aluminium oxide and copper oxide (Al_2O_3-CuO) nanoparticles, are considered. Ethylene glycol is used as base fluid in both cases.
- Non-linear convection and viscous dissipation are taken into consideration to explore flow and heat transfer characteristics.

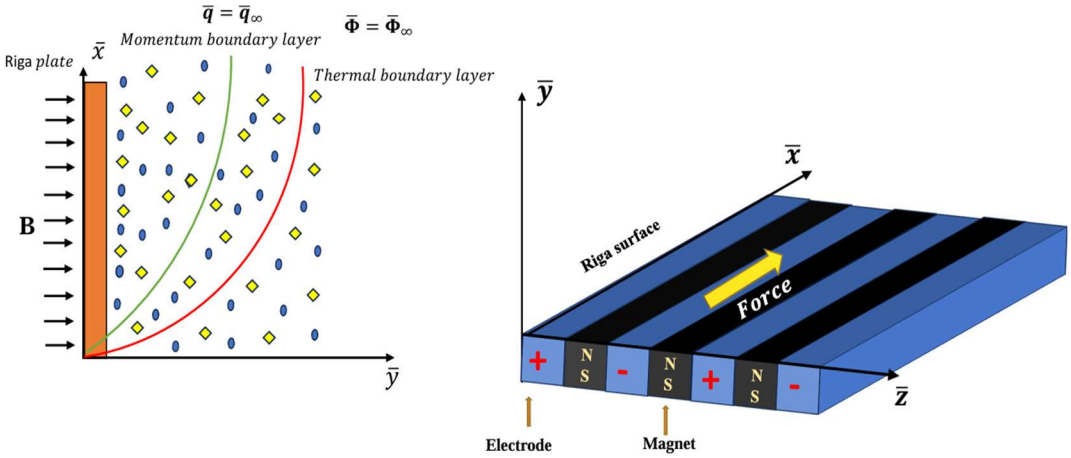

Fig.1. Schematic diagram of the flow.

2. Mathematical formulation of the problem

Unsteady MHD flow and thermal transport properties of hybrid nanofluids near a Riga plate is examined. Two types of hybrid nanofluid, consisting nanoparticles, namely, (i) silver and gold ($Ag-Au$) and

(ii) alumina and copper oxide $\left(Al_2O_3 - CuO\right)$ in base fluid Ethylene glycol, is considered. Flow and heat transfer analysis is carried out by incorporating the characteristics of non-linear convection and viscous dissipation. Flow field is generated by impulsive movement of Riga plate. $\bar{\Phi}_S$ and $\bar{\Phi}_\infty$ are values of fluid temperature at the surface and outside of the boundary layer region. A sketch of flow problem is depicted in Fig.1. Equations (2.1)-(2.2) are governing equations of flow system in vector form.

$$\rho_4 \partial_{\bar{t}} \vec{V} + (\vec{V}\cdot\nabla)\vec{V} = \nabla\Omega_{xy} + \vec{J}\times\vec{B} + \frac{\pi j_0 M_0}{8} e^{-\pi a^{-1}\bar{y}} + g\left\{\Lambda_L\left(\bar{\Phi}-\bar{\Phi}_\infty\right) + \Lambda_N\left(\bar{\Phi}-\bar{\Phi}_\infty\right)^2\right\}\rho_4, \quad (2.1)$$

$$\left(\rho c_p\right)_4 \partial_{\bar{t}} T = k_4 \nabla^2 T + \mu_4 (1+l_r)^{-1}\left\{\nabla\bar{q}\cdot\nabla\bar{q} + l_w\left(\nabla\bar{q}\right)\left(\partial_{\bar{t}}\nabla\bar{q}\right)\right\} \quad (2.2)$$

where $\Omega_{xy} = \frac{\mu_4}{(1+l_r)}\left(1 + l_w\frac{\partial}{\partial\bar{t}}\right)\frac{\partial\bar{q}}{\partial\bar{y}}$, is the non-trivial tangential stress.

Equations (2.3) and (2.6), represent the heat and flow system in mathematical language,

$$\begin{aligned}\rho_4\partial_{\bar{t}}\bar{q} = \mu_4\left(1+l_r\right)^{-1}\left(1+l_w\partial_{\bar{t}}\right)\partial_{\bar{y}}^2\bar{q} - \sigma_4 B^2\bar{q} + \frac{\pi j_0 M_0}{8}e^{-\pi a^{-1}\bar{y}} + \\ + g\left\{\Lambda_L\left(\bar{\Phi}-\bar{\Phi}_\infty\right) + \Lambda_N\left(\bar{\Phi}-\bar{\Phi}_\infty\right)^2\right\}\rho_4,\end{aligned} \quad (2.3)$$

$$\left(\rho c_p\right)_4 \partial_{\bar{t}}\bar{\Phi} = k_4\partial_{\bar{y}}^2\bar{\Phi} + \mu_4(1+l_r)^{-1}\left\{\left(\partial_{\bar{y}}\bar{q}\right)^2 + l_w\left(\partial_{\bar{y}}\bar{q}\right)\left(\partial_{\bar{t}\bar{y}}^2\bar{q}\right)\right\}. \quad (2.4)$$

Boundary conditions:

$$\left.\begin{aligned}\bar{q} &= 0\\ \bar{\Phi} &= 0\end{aligned}\right\} \forall\,\bar{y}, \quad \text{when} \quad \bar{t} = 0, \quad (2.5)$$

$$\left.\begin{aligned}&\bar{q} = q_0, \quad -k_4\partial_y\bar{\Phi} = h_1\left(\bar{\Phi}_S - \bar{\Phi}\right): && \text{at} \quad \bar{y} = 0\\ &\bar{q}\to 0, \quad \bar{\Phi}\to\bar{\Phi}_\infty: && \text{as} \quad \bar{y}\to\infty\end{aligned}\right\} \bar{t} > 0\,. \quad (2.6)$$

The thermophysical properties of the hybrid nanofluid in mathematical form are listed in Tab.2.

Table 2. Thermal properties like density, viscosity, heat capacity and thermal conductivity of hybrid nanofluids. ([41], [42]).

$\rho_4 = p_2\rho_2 + p_3\rho_3 + (1-p_4)\rho_1 \quad$ where $\quad p_4 = p_2 + p_3\,,$
$\mu_4 = \mu_1 \big/ \left(1 - p_2 - p_3\right)^{2.5}\,,$
$\left(\rho\beta_T\right)_4 = p_2\left(\rho\beta_T\right)_2 + p_3\left(\rho\beta_T\right)_3 + (1-p_4)\left(\rho\beta_T\right)_1\,,$
$\left(\rho C_p\right)_4 = p_2\left(\rho C_p\right)_2 + p_3\left(\rho C_p\right)_3 + (1-p_4)\left(\rho C_p\right)_1\,,$
$\frac{k_4}{k_1} = \frac{\left(k_4+2k_1\right) - 2p_4\left(k_1-k_4\right)}{\left(k_4+2k_1\right) + p_4\left(k_1-k_4\right)} \quad$ where $\quad k_4 = \frac{\left(p_2k_2 + p_3k_3\right)}{p_2+p_3}\,.$

Equations (2.3)-(2.6) are non-dimensionalised and kept in the same form by making use of following set of transformations.

$$q=\bar{q}/q_0,\quad t=\bar{t}q_0^2/\nu_1,\quad y=\bar{y}q_0/\nu_1,\quad \Phi=\left(\bar{\Phi}-\bar{\Phi}_\infty\right)(\nabla\theta)^{-1},\quad \nabla\theta=\left(\bar{\Phi}_s-\bar{\Phi}_\infty\right). \tag{2.7}$$

Transformed equations are

$$e_1(1+l_r)^{-1}\left(\partial_y^2 q+l\partial_{tyy}^3 q\right)-e_2Hq+Qe^{-\beta y}+e_3Gr\Phi\left(1+G^*\Phi\right)-e_0\partial_t q=0, \tag{2.8}$$

$$e_5\partial_y^2\Phi+e_1\,\mathrm{Pr}\,Ec\left(1+l_r\right)^{-1}\left\{\left(\partial_y q\right)^2+l\left(\partial_y q\right)\left(\partial_{ty}^2 q\right)\right\}-e_4\,\mathrm{Pr}\,\partial_t q=0 \tag{2.9}$$

where

$$e_0=\frac{(p_2\rho_2+p_3\rho_3)}{\rho_1}+\left(1-p_2-p_3\right),\qquad e_1=\left(1-p_2-p_3\right)^{2.5},$$

$$e_2=1+\frac{3\left(\dfrac{p_2\sigma_2+p_3\sigma_3}{\sigma_1}\right)-3\left(p_2+p_3\right)}{2\left(\dfrac{p_2\sigma_2+p_3\sigma_3}{(p_2+p_3)\sigma_1}\right)-\left(\dfrac{p_2\sigma_2+p_3\sigma_3}{\sigma_1}-p_2-p_3\right)},$$

$$e_3=\frac{p_2\left(\rho\Lambda_L\right)_2+p_3\left(\rho\Lambda_N\right)_3}{\left(\rho\Lambda_L\right)_1}+\left(1-p_2-p_3\right),\qquad e_4=\frac{p_2\left(\rho c_p\right)_2+p_3\left(\rho c_p\right)_3}{\left(\rho c_p\right)_1}+\left(1-p_2-p_3\right),$$

$$e_5=\frac{\left(k_{23}+2k_1\right)-2\left(p_2+p_3\right)\left(k_1-k_{23}\right)}{\left(k_{23}+2k_1\right)+\left(p_2+p_3\right)\left(k_1-k_{23}\right)},\qquad k_{23}=\frac{p_2k_2+p_3k_3}{p_2+p_3}.$$

Table 3. Values of physical parameters of base fluid and nanoparticles. ([42], [43]).

Physical Properties	**Base fluid**	**Nanoparticles**			
	Ethylene glycol $C_2H_6O_2$	Silver (Ag)	Gold (Au)	Aluminium Oxide (Al_2O_3)	Copper Oxide (CuO)
$\rho(kg/m^3)$	*1115*	*10500*	*19300*	*3970*	*6500*
$C_p(J/kgK)$	*2386*	*235*	*129.1*	*765*	*533*
$K(W/mK)$	*0.2499*	*429*	*318*	*40*	*17.65*
$\beta(k^{-1})$	5.7×10^{-5}	1.89×10^{-5}	1.4×10^{-5}	0.85×10^{-5}	1.8×10^{-5}
$\sigma(S/m)$	10.7×10^{-5}	6.30×10^{7}	4.24×10^{7}	35×10^{6}	69×10^{-2}
Pr	*21*	-	-	-	-
μ (cP)	*18.376*				

Prandtl number of the ethylene glycol is at $263K$ and other considered values are at room temperature i.e $293K$. Associated boundary conditions will become:

$$\left.\begin{aligned} &q(y,0)=0, \quad \Phi(y,0)=0, \\ &q(0,t)=1, \quad q(\infty,t)\to 0, \quad \Phi(\infty,t)\to 0, \\ &e_5\partial_y\Phi(0,t)=-\gamma^*\left(1-\Phi(0,t)\right), \end{aligned}\right\} \tag{2.10}$$

where

$$l=l_w q_0^2/\nu_1, \quad H=\sigma_1 B_0^2\nu_1/\rho_1 q_0^2, \quad \beta=\pi\nu_1/aq_0, \quad Q=\pi j_0 M_0\nu_1/8q_0^3,$$

$$G^*=\left(\frac{\Lambda_N}{\Lambda_L}\right)(\nabla\theta), \quad Pr=\nu_1/\alpha_1, \quad Ec=q_0^2\left(c_p\nabla\theta\right)^{-1}.$$

3. Solution technique

Since the equations (2.8) and (2.9) are coupled and nonlinear, an analytical solution is typically difficult to discover. Here, we will apply the SQLM approach to solve the system (2.8) and (2.9) numerically under the given initial and boundary conditions (2.10). Initially, it is assumed that the system consists of distinct equations for q and Φ in order to force the system of equations to be solved. In order to linearize the solved equations, a quasilinearization method using Taylor series expansion is applied. This is because the approximate solutions of each function and their derivatives at the $(r+1)^{th}$ and r^{th} levels of iteration differ slightly. The linear resolved system of equations is solved by using the Chebyshev spectral collocation method. The nonlinear terms in the system of equations (2.8) and (2.9) are

$$\Phi^2, \left(\partial_y q\right)^2, \partial_y q\partial_{ty}^2 q,$$

First, we convert equations (2.8) and (2.9) into quasilinear form as follows:

$$\begin{aligned} &[z_0]q''_{r+1}+[z_1]q_{r+1}+[z_2]\Phi_{r+1}=-[z_3]\partial_t q''_{r+1}-[z_4]\partial_t q_{r+1}+[z_5], \\ &[z_6]\Phi''_{r+1}+[z_7]q'_{r+1}=-[z_8]\partial_t\Phi-[z_9]\left(\partial_t q'\right)_{r+1}+[z_{10}], \end{aligned} \tag{3.1}$$

where the subscripts $r+1$ and r denote the iteration levels for the current and prior iterations, respectively.

$$z_0=e_1/(1+l_r), \quad z_1=-e_2H, \quad z_2=e_3G_r+2e_3GrG^*\Phi_r, \quad z_3=-\left(\left(e_1/(1+l_r)\right)\right)l,$$

$$z_4=e_0, \quad z_5=Qe^{-\beta y}+e_3GrG^*\Phi_r^2, \quad z_6=e_5\left(Pr\right)^{-1},$$

$$z_7=2\left(e_1Ec/\left(1+l_r\right)\right)q'_r+\left(e_1Ec/\left(1+l_r\right)\right)l\left(\partial_t q'\right)_r, \quad z_8=e_4,$$

$$z_9 = le_1 Ec\left(1+l_r\right)^{-1} q_r^{'}, \quad z_{10} = e_1 Ec\left(1+l_r\right)^{-1}\left[q_r^{'2} + l\left(\partial_t q'\right)_r q_r^{'}\right].$$

Time and space domain are mapped to $\left[-1,1\right]$ using linear transformation to apply Chebyshev collocation spectral technique to the system (3.1) and (3.2). The range $[-1,1]$ is discretized by considering Gauss Labatto points $\left(y_\alpha, t_\beta\right), \alpha = 0,1,2,\ldots,N_s, \beta = 0,1,2,\ldots,N_t$, N_s and N_t being number of grid points along space and time directions. Solutions are derived by making use of bivariate Lagrange interpolation polynomials, given by

$$V\left(y,t\right) \approx \sum_{\alpha=0}^{N_s}\sum_{\beta=0}^{N_t} V\left(y_\alpha, t_\beta\right)\Omega_\alpha\left(y\right)\Omega_\beta\left(t\right), V = \left(q,\Phi\right).$$

This polynomial gives the values of fluid velocity and temperature at grid points i.e., Gauss-Lobatto collocation points,

$$y_k = cos\left(\frac{\pi k}{N}\right), \quad k = 0,\ 1,\ 2,\ \ldots, N.$$

$$\left.\frac{\partial^m V}{\partial y^m}\right|_{(y_\alpha, t_\beta)} = \boldsymbol{D}^m \boldsymbol{V}, \quad m = 1,2,3\,, \left.\frac{\partial V}{\partial t}\right|_{(y_\alpha, t_\beta)} = \sum_{\beta=0}^{N_t} \boldsymbol{d}_{\alpha\beta} \boldsymbol{V}_\beta,$$

$\boldsymbol{D}$ and $\boldsymbol{d}$ are matrices of order $\left(N_s+1\right)\times\left(N_s+1\right)$ and $\left(N_t+1\right)\times\left(N_t+1\right)$ respectively, termed as Chebyshev differentiation matrices with respect to space and time variable. Thus, V represents

$$V = \left[V\left(y_0\right), V\left(y_1\right),\ldots, V\left(y_{N_s}\right)\right]^T.$$

By essence of multi-domain method, the time domain $\lambda = \left[0,T\right]$ is partitioned into non-overlapping intervals $\lambda_p = \left[t_{p-1}, t_p\right], p = 1,2,\ldots,T.$ Solution of the system (3.1) and (3.2) in the first segment i.e., $[t_0, t_1]$ are fetched using given initial solution. Computed solution at λ_{p-1} segment will serve as initial conditions while working for solution in subsequent segments λ_p, this way, we achieve the solution in each segments i.e. whole time span. The following relation emphasize the continuity behaviour,

$$V^{(\delta)}\left(y, t_{\delta-1}\right) = V^{(\delta-1)}\left(y, t_{\delta-1}\right),$$

Multi-domain approach on system (3.1) and (3.2) takes the form

$$\left[z_0^{(\delta)}\right] q_{r+1}^{''(\delta)} + \left[z_1^{(\delta)}\right] q_{r+1}^{(\delta)} + \left[z_2^{(\delta)}\right] \Phi_{r+1}^{(\delta)} = -\left[z_3^{(\delta)}\right] \partial_t q_{r+1}^{''(\delta)} + \left[z_4^{(\delta)}\right] \partial_t q_{r+1}^{(\delta)} + \left[z_5^{(\delta)}\right], \tag{3.3}$$

$$\left[z_6^{(\delta)}\right] \Phi_{r+1}^{''(\delta)} + \left[z_7^{(\delta)}\right] q_{r+1}^{'(\delta)} = \left[z_8^{(\delta)}\right] \partial_t \Phi_{r+1}^{(\delta)} - \left[z_9^{(\delta)}\right]\left(\partial_t q_{r+1}^{\prime(\delta)}\right)_{r+1} + \left[z_{10}^{(\delta)}\right]. \tag{3.4}$$

System of equations (3.3) and (3.4) after implementing Chebyshev spectral method, we obtain

$$\boldsymbol{A}_{11,i}^{(\delta)}\left(\boldsymbol{q}\right)_{r+1,i}^{(\delta)}+\boldsymbol{A}_{12,i}^{(\delta)}\left(\boldsymbol{\Phi}\right)_{r+1,i}^{(\delta)}+\left[z_3^{(\delta)}\right]\sum_{j=0}^{N_t}\boldsymbol{d}_{i,j}\boldsymbol{D}^2\boldsymbol{q}_{r+1,j}^{(\delta)}-\left[z_4^{(\delta)}\right]\sum_{j=0}^{N_t}\boldsymbol{d}_{i,j}\boldsymbol{q}_{r+1,j}^{(\delta)}=\boldsymbol{R}_{1,i}^{(\delta)},$$

$$\boldsymbol{A}_{21,i}^{(\delta)}\left(\boldsymbol{q}\right)_{r+1,i}^{(\delta)}+\boldsymbol{A}_{22,i}^{(\delta)}\left(\boldsymbol{\Phi}\right)_{r+1,i}^{(\delta)}+\left[z_8^{(\delta)}\right]\sum_{j=0}^{N_t}\boldsymbol{d}_{i,j}\boldsymbol{D}\boldsymbol{q}_{r+1,j}^{(\delta)}-\sum_{j=0}^{N_t}\boldsymbol{d}_{i,j}\boldsymbol{\Phi}_{r+1,j}^{(\delta)}=\boldsymbol{R}_{2,i}^{(\delta)}$$

where

$$\boldsymbol{A}_{11,i}^{(\delta)}=\left(z_0^{\delta}\right)\boldsymbol{D}^2+\left(z_1^{\delta}\right)\boldsymbol{I},\quad \boldsymbol{A}_{12,i}^{(\delta)}=\left(z_2^{\delta}\right)\boldsymbol{I},\quad \boldsymbol{A}_{21,i}^{(\delta)}=\left(z_6^{\delta}\right)\boldsymbol{D},$$

$$\boldsymbol{A}_{22,i}^{(\delta)}=\left(z_7^{\delta}\right)\boldsymbol{D}^2,\quad \boldsymbol{R}_{1,i}^{(\delta)}=\left(z_5^{\delta}\right)-\left(z_3^{\delta}\right)d_{i,N_{t+1}}D^2q_{i,N_{t+1}}+\left(z_3^{\delta}\right)d_{i,N_{t+1}}q_{i,N_t+1},$$

$$\boldsymbol{R}_{2,i}^{(\delta)}=\left(z_{10}^{\delta}\right)-\left(z_8^{\delta}\right)d_{i,N_{t+1}}Dq_{i,N_{t+1}}+\left(z_8^{\delta}\right)d_{i,N_{t+1}}\Phi_{i,N_{t+1}}$$

and I is an identity matrix of size $\left(N_S+1\right)\times\left(N_S+1\right)$.

4. Convergence and accuracy

This section explains both convergence and accuracy of the solution achieved using the SQLM. The following parameter values are considered to compute solution and residual errors: $l_r=1, l=1$, $G^*=0.002$, $H=1, Gr=2, Q=0.5$, $\beta=0.1$, $\gamma^*=0.1, Ec=0.02$ and $t=0.4$. Solution and residual errors are displayed in Figs 2-7. Twenty grid points in t (time) and eighty in y (space) directions are used. The grid-independent test results demonstrated their ability to yield precise solutions.

4.1. Solution errors

When $l_r=1, l=1$, $G^*=0.002$, $H=1, Gr=2, Q=0.5$, $\beta=0.1$, $\gamma^*=0.1, Ec=0.02$ and $t=0.4$. Convergence of the solution is shown by calculating infinite norm of the deviation in solutions between two consecutive iterations. This measure is referred as solution error.

$$\left\|q\right\|_{\infty}=\max_{0\le i\le N_S}\left\|q_{r+1,i}-q_{r,i}\right\|_{\infty},\tag{4.1.1}$$

$$\left\|\Phi\right\|_{\infty}=\max_{0\le i\le N_S}\left\|\Phi_{r+1,i}-\Phi_{r,i}\right\|_{\infty}.\tag{4.1.2}$$

When the deviation in solution between consecutive iteration tends to zero, suggesting that further iterations will not affect the solutions, the SQLM method is said to have converged. Figures 2 and 3 present the errors in solving the system of PDEs. The errors decrease steadily with more iterations, demonstrating the convergence of this approach. The error quickly falls to 10^{-14} after just a few iterations for q and stays consistent, whereas it takes approximately 4 iterations for Φ to reach tolerance level of 10^{-16}. This analysis of solution errors demonstrates that the method converges quickly in a relatively small number of iterations.

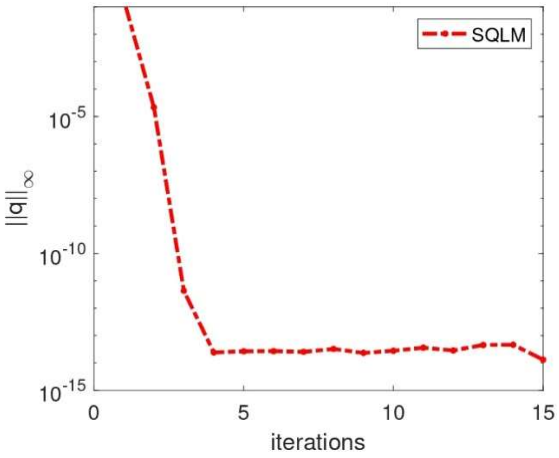

Fig.2. Solution error of q with iteration.

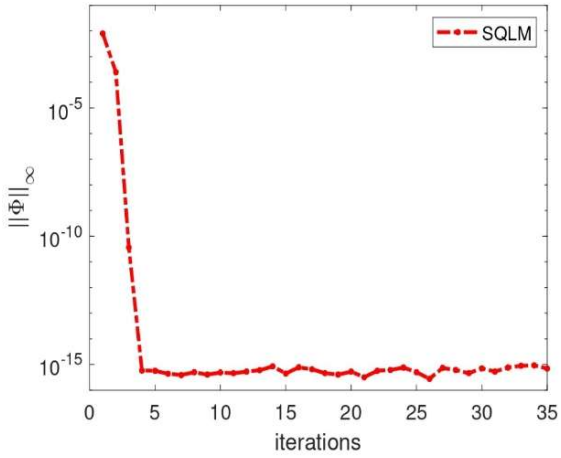

Fig.3. Solution error of Φ with iteration.

4.2. Residual errors

When $l_r = 1, l = 1$, $G^* = 0.002$, $H = 1$, $Gr = 2$, $Q = 0.5$, $\beta = 0.1$, $\gamma^* = 0.1$, $Ec = 0.02$. The exactness of solutions obtained by SQLM approach is assessed using the residual error norms derived by putting the approximate solution in the original system of differential Eqs (2.8) and (2.9). Figures 4 to 7 show the residual error. The residual error shows a rapid drop in Figs 4 to 7, suggesting that the approximate solution is reasonably near to the actual solution. This is sufficient to verify the accuracy of the estimated approximate solution. We can conclude that, for models of a comparable kind, the solution method SQLM yields fairly accurate approximate results. The residual errors of the obtained numerical solutions approach to 10^{-13} accuracy shortly after a few iterations in q and Φ as shown in Figs 4 to 7. Figures 6 and 7 demonstrate that the error reduces to 10^{-13} in just 0.1 seconds.

$$\mathrm{Re}s(q) = \max_{0 \le i \le N_S} \left\| e_1 (1 + l_r)^{-1} \left(\partial_y^2 q + l \partial_{tyy}^3 q \right) - e_2 H q + Q e^{-\beta y} + e_3 Gr \Phi \left(1 + G^* \Phi \right) - e_0 \partial_t q \right\|_\infty, \quad (4.2.1)$$

$$\mathrm{Re}s(\Phi) = \max_{0 \le i \le N_S} \left\| e_5 \partial_y^2 \Phi + e_1 \Pr Ec \left(1 + l_r \right)^{-1} \left\{ \left(\partial_y q \right)^2 + l \left(\partial_y q \right) \left(\partial_{ty}^2 q \right) \right\} - e_4 \Pr \partial_t q \right\|_\infty. \quad (4.2.2)$$

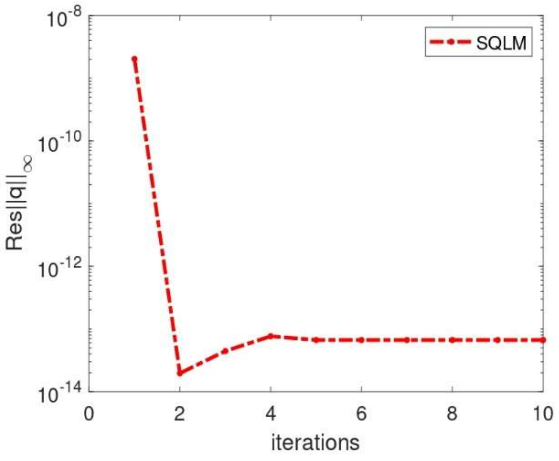

Fig.4. Residual error of q with iteration.

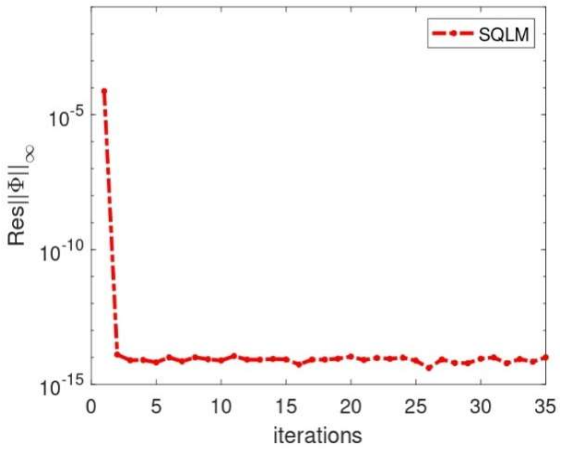

Fig.5. Residual error of Φ with iteration.

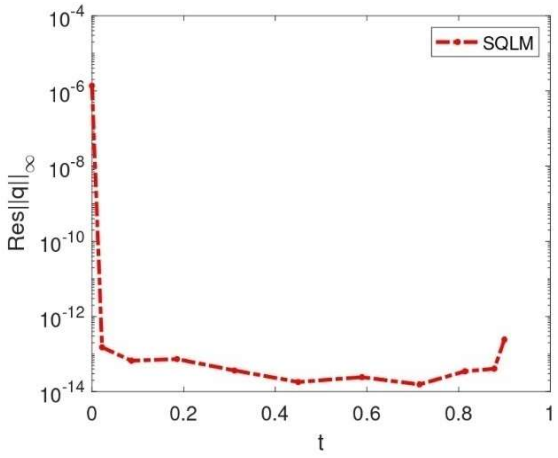

Fig.6. Residual error of q with t.

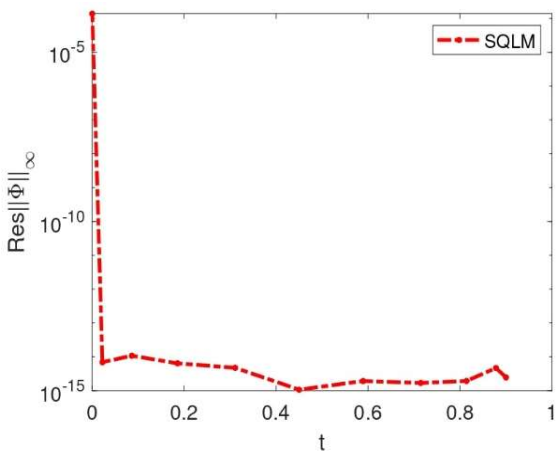

Fig.7. Residual error of Φ with t.

5. Results and discussion

The numerical results, to governing partial differential equations derived by SQLM, are presented in graphical and tabular form. An overview of physics linked to the influence of significant flow parameters on dimensionless velocity q and temperature Φ, is discussed to explore heat and flow behaviour. Figures are sketched by considering the parameter's values as follows $l_r = 1$, $l = 1$, $G^* = 0.002$, $H = 1$, $Gr = 2$, $Q = 0.2$, $\beta = 0.1$, $\gamma^* = 0.1$ and $Ec = 0.02$. These parameter values are in line with the values present in literature.

Figures 8 and 9 are plotted to elucidate the impact of rising Hartmann number on the velocity and temperature profile. Figure 8 demonstrates that rising H reduces fluid velocity in both hybrid nanoliquids. This decline in fluid velocity happens as a result of resistive forces generated within the fluid with greater values of H. Figure 9 shows that Hartman number exerts an uprising influence in fluid temperature near the surface. A comparison of given two hybrid nanoliquids reveals that hybrid nanoliquid $(Al_2O_3 - CuO)/C_2H_6O_2$ performs better in terms of thermal presentation compared $(Ag - Au)/C_2H_6O_2$.

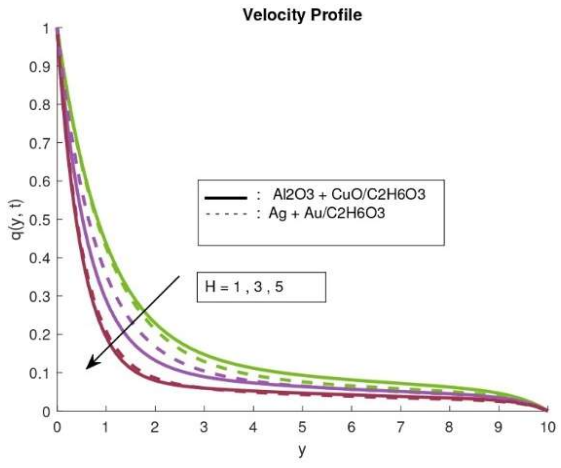

Fig.8. Variation in velocity with H.

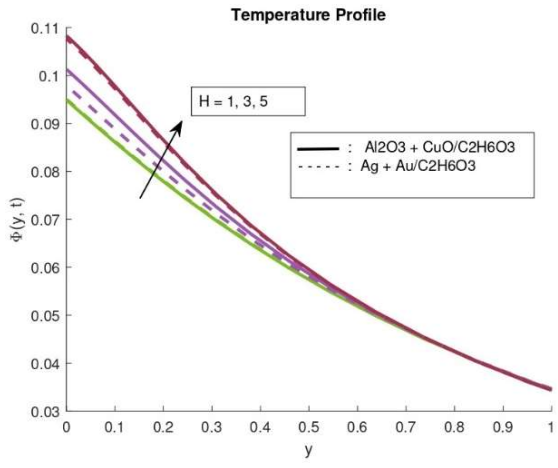

Fig.9. Temperature for different H.

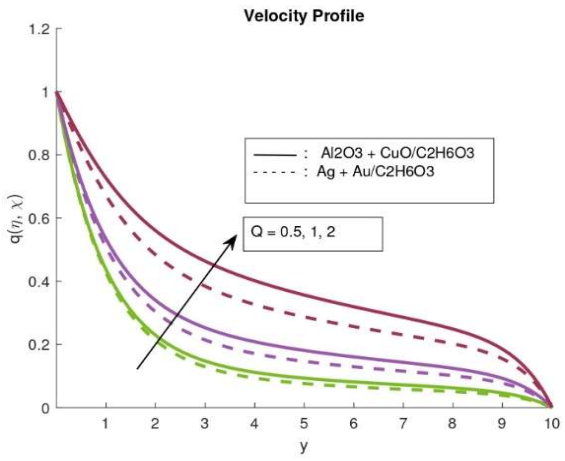

Fig.10. Variation in velocity with *Q*.

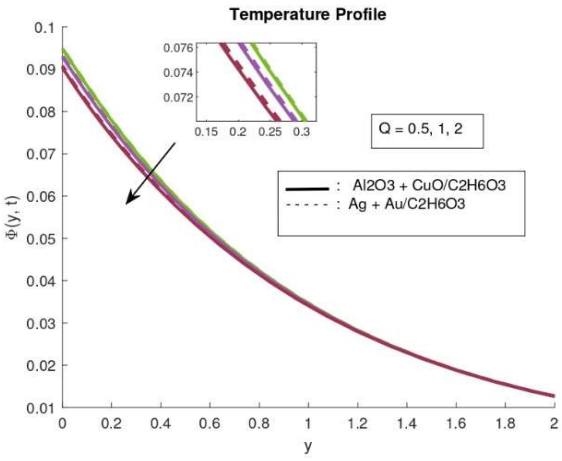

Fig.11. Temperature for different values of *Q*.

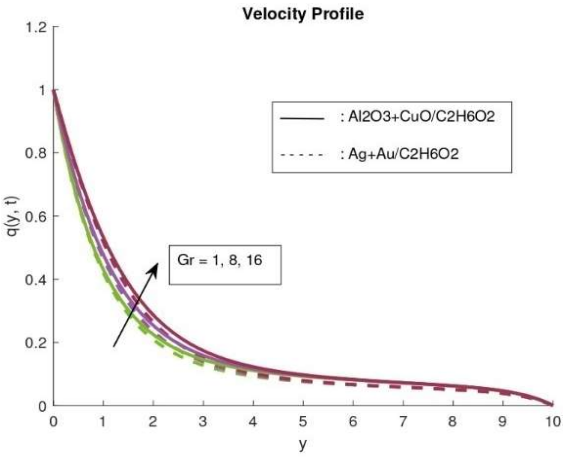

Fig.12. Velocity with *Gr*.

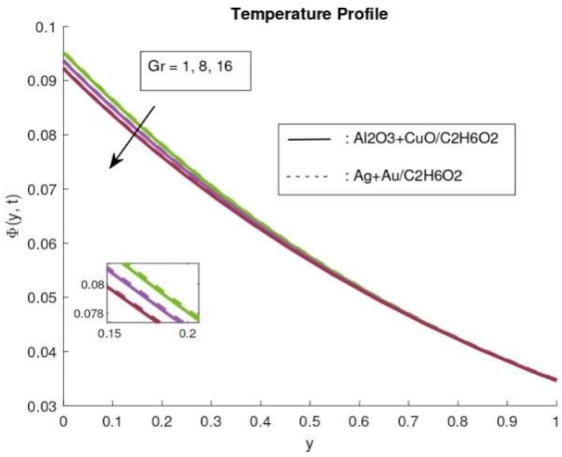

Fig.13. Temperature with *Gr*.

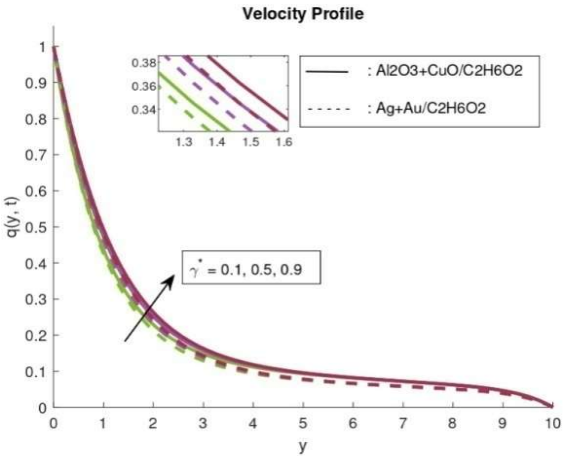

Fig.14. Variation in velocity with γ^*.

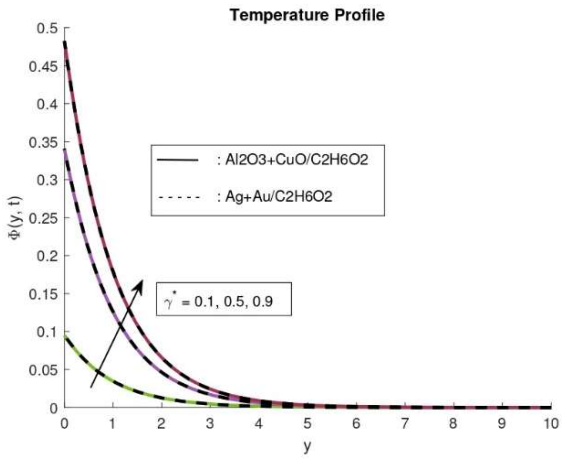

Fig.15. Temperature for different γ^*.

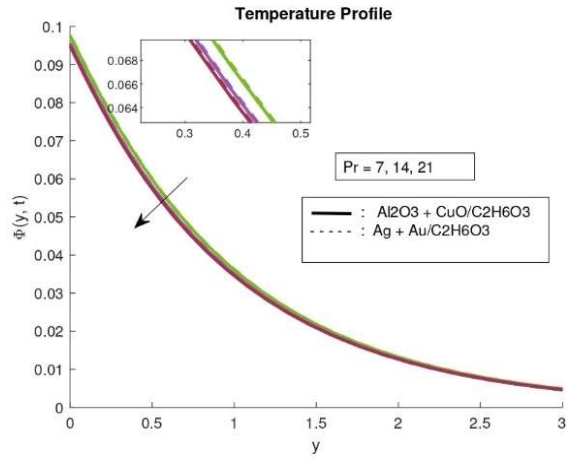

Fig.16. Temperature profile with Pr.

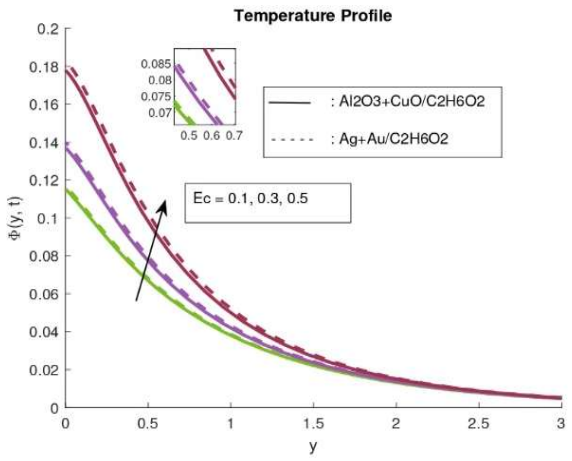

Fig.17. Temperature profiles with Ec.

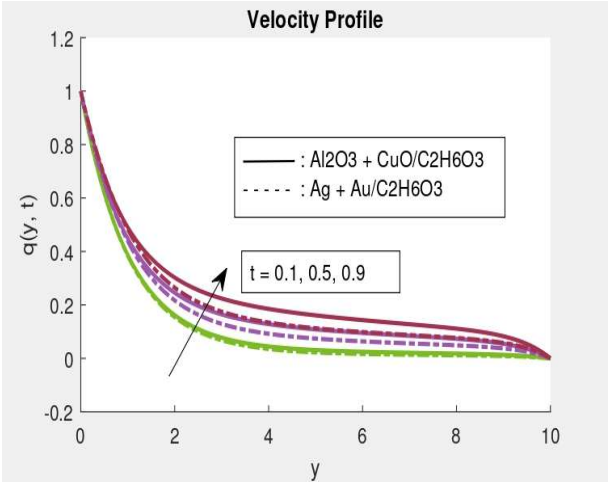

Fig.18. Variation in velocity profile for time t.

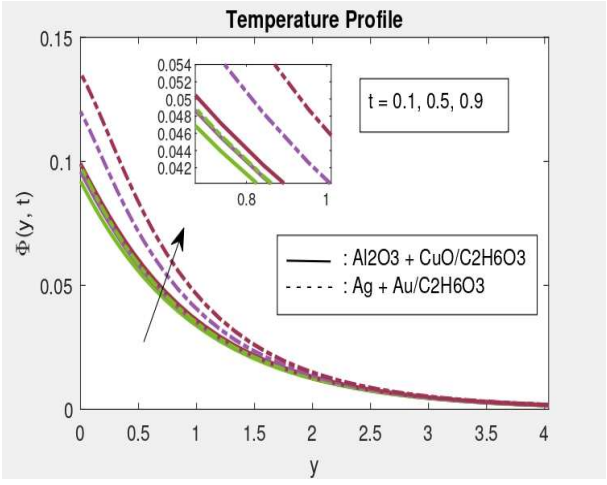

Fig.19. Temperature profile with time t.

The impact of the modified Hartman number Q is shown in Figs 10 and 11. Increasing Q leads to the elevation of fluid velocity but diminishing temperature in the boundary layer region. This is evident because of the fact that Riga plate produces electromagnetic waves and this electromagnetic force acts along the fluid motion, this helps to enhance fluid velocity and heat transfer rate in both the models. It is worth noting that $(Al_2O_3 - CuO)/C_2H_6O_2$ performs better than $(Ag - Au)/C_2H_6O_2$ in elevating the fluid velocity and the heat transfer rate within the boundary layer.

The ratio of buoyant force to viscous force is termed as the Grashof number. Figures 12 and 13 illustrate an interesting impact of Gr (thermal buoyancy factors) on the resultant velocity and temperature profiles. Fluid velocity grows as Gr improves. Consequently, as the magnitude of thermal Gr rises, so does the heat transfer rate near the surface. Higher values of Grashof number refer a stronger buoyancy force. The fluid velocity rises as a result, the resulting momentum boundary layer thickness improves which exerts an increasing influence on the rate of heat transfer in both the scenarios. It is noticed that $(Al_2O_3 - CuO)/C_2H_6O_2$ performs better than $(Ag - Au)/C_2H_6O_2$ in both in enhancing fluid flow and heat transfer rate.

Figures 14 and 15 demonstrate how the velocity and temperature profiles are affected by thermal Biot number. Elevated fluid velocity and temperature profiles close to the boundary are indicated by an improvement in convective heat transfer coefficient. To maintain the free stream values, the temperature and

fluid velocity diminish uniformly. Biot number measures a significant change in temperature inside a body in space, hence, this fact leads a significant improvement in fluid temperature with augmenting values of Biot number. Thermal behaviour of both hybrid nanofluid are almost same.

The impact of Pr on the temperature distribution of nano liquid is seen in Fig.16. Expanding values of Pr convey a nominal reduction in fluid temperature. Pr stands for momentum to thermal diffusivity ratio. Figure 17 shows the impact of Eckert number Ec on temperature profiles of hybrid nanofluids. Improving Ec magnitude enhances the thermal boundary layer. Temperature of nanofluid rises significantly with Ec in the boundary layer and then drops towards free stream temperature value far from the surface. The Ec is essentially the kinetic energy to enthalpy ratio.

Figures 18 and 19 summarize the time-dependent response of fluid velocity and temperature. These figures show how momentum and thermal boundary layers grow over time. A growing nature in fluid velocity and temperature with time is revealed in Figs 18 and 19. The increase in fluid velocity is more pronounced at a little away from the Riga surface and hence, it shows a reduction in boundary layer separation.

The values of drag coefficient (skin friction) and heat transfer coefficient (Nusselt number) is depicted in Tabs 4 and 5 for varying Hartmann number, modified Lorentz force, Grashof number, thermal Biot number, Eckert number and time.

Table 4. Table of skin friction and Nusselt number for $(Ag-Au)/C_2H_6O_2$ when $l_r=1,\ l=1,\ G^*=0.002,\ H=1, Gr=1, Q=0.5,\ \beta=0.1,\ \gamma^*=0.1,\ Ec=0.02,\ t=0.1.$

H	Q	Gr	γ^*	Ec	t	Cf_x	Nu_x
1						0.908827	0.090490
3						1.162164	0.090205
5						1.810016	0.089230
	0.5					0.908827	0.090490
	1					0.734581	0.090665
	2					0.385966	0.090917
		1				0.932379	0.090466
		8				0.768280	0.090622
		16				0.582701	0.090768
			0.1			0.908827	0.090490
			0.5			0.784843	0.329672
			0.9			0.713028	0.465657
				0.1		0.906471	0.089518
				0.3		0.900649	0.087163
				0.5		0.894924	0.084912
					0.1	0.970411	0.090182
					0.5	0.859632	0.087992
					0.9	0.761826	0.086438

Table 5. Table of skin friction and Nusselt number for $(Al_2O_3-CuO)/C_2H_6O_2$ when $l_r=1,\ Q=0.5,\ l=1, G^*=0.002,\ Gr=1,\ \beta=0.1, \gamma^*=0.1,\ Ec=0.02$ and $t=0.1.$

H	Q	Gr	γ^*	Ec	t	Cf_x	Nu_x
1						0.900112	0.090507
3						1.415737	0.089868
5						1.844124	0.089169
	0.5					0.900112	0.090507
	1					0.706829	0.090698
	2					0.320109	0.090957
		1				0.922983	0.090484
		8				0.763601	0.090635
		16				0.583288	0.090777
			0.1			0.900112	0.090507
			0.5			0.779570	0.329765
			0.9			0.709748	0.465830
				0.1		0.898029	0.089594
				0.3		0.892877	0.087375
				0.5		0.887805	0.085246
					0.1	0.972189	0.090794
					0.5	0.883283	0.090410
					0.9	0.821371	0.090087

6. Conclusion

A study on Jeffery hybrid nanofluid flow and heat transfer over an impulsive moving surface with electromagnetic hydrodynamic properties with nonlinear convection is performed. Two hybrid nanofluids: $(Al_2O_3-CuO)/C_2H_6O_2$ and $(Ag-Au)/C_2H_6O_2$ are considered for analysis. The heat transfer in the flow system is influenced by various factors, such as magnetic field, modified Lorentz force, viscous dissipation and nonlinear convection. We exercised the spectral quasi-linearization method (SQLM) to generate the

accurate solution. The accuracy of achieved results is analysed. The results are reproduced in graphical and tabular form. This study reveals the following. Fluid temperature augments with the rise in Hartmann number H. Modified Hartmann number Q and Grashof number Gr intensify velocity of hybrid nanofluid. An inverse relationship between the modified Hartmann number and the temperature profile is noticed. The temperature profile drops uniformly within the boundary layer until it reaches the free stream value as Gr grows. Growing thermal Biot number improves both velocity and temperature profiles. Higher values of Eckert number produce a rise in fluid temperature.

To wrap up our findings, we can assert after accomplishing comparative analysis that the hybrid nanofluid $\left(Al_2O_3 - CuO\right)/C_2H_6O_2$ outshines the hybrid nanofluid $\left(Ag - Au\right)/C_2H_6O_2$ in boosting fluid flow and amplifying the heat transfer rate under these conditions and configuration.

Nomenclature

a – width of magnets between electrodes
B – applied magnetic field strength
c_p – specific heat capacity
Ec – Eckert number
G^* – non-linear thermal convection parameter
Gr – Grashof number
g – acceleration due to gravity
H – Hartmann number
h_1 – convective heat transfer coefficient
j_0 – current density in electrode
k – thermal conductivity
l – material parameter
l_r – ratio of relaxation to retardation time
l_w – retardation time
M_0 – magnetization of magnets mounted on the surface of Riga plate
Pr – Prandtl number
p_2 – fraction of first nanoparticles
p_3 – fraction of second nanoparticles
Q – modified Hartmann number
q – dimensionless velocity
$\overline{q}$ – dimensional velocity
t – time
β – a dimensionless parameter
γ^* – Biot number
Λ_L – linear thermal expansion
Λ_N – non-linear thermal expansion coefficient
μ – viscosity
ρ – density
σ – electrical conductivity

Φ – dimensionless temperature

$\bar{\Phi}$ – dimensional temperature

subscripts

1 – for base fluid

2 – for first nanoparticles

3 – for second nanoparticles

4 – for hybrid nanoliquid

s – at surface

∞ – away from the boundary layer region

References

[1] Choi S.U.S. and Eastman J.A. (1995): *Enhancing thermal conductivity of fluids with nanoparticles*.– ANL/MSD/CP-84938; CONF-951135-29. Argonne National Lab.(ANL), Argonne, IL (United States).

[2] Alrabaiah H., Bilal H.M., Khan M.A., Muhammad T. and Legas E.Y. (2021): *Time fractional model of electro-osmotic Brinkman-type nanofluid with heat generation and chemical reaction effects: Application in cleansing of contaminated water*.– Scientific Reports, vol.11, No.24402, https://doi.org/10.1038/s41598-021-03062-9.

[3] Molana M., Ghasemiasl R. and Armaghani T. (2022): *A different look at the effect of temperature on the nanofluids thermal conductivity: focus on the experimental-based models*.– J. Thermal Analysis and Calorimetry, vol.147, pp.4553-4577, https://doi.org/10.1007/s10973-021-10836-w.

[4] Alagumalai A., Qin C., Vimal K.E.K., Solomin E., Yang L., Zhang P., Otanicar T., Kasaeian A., Chamkha A.J., Rashidi M.M., Wongwises S., Ahn H.O., Lei Z., Saboori T. and Mahian O. (2022): *Conceptual analysis framework development to understand barriers of nanofluid commercialization*.– Nano Energy, vol.92, No.106736, https://doi.org/1 0.1016 /j.nanoen. 2021.106736.

[5] Arif M., Ali F., Sheikh N.A. and Khan I. (2019): *Enhanced heat transfer in working fluids using nanoparticles with ramped wall temperature: applications in engine oil*.– Advances in Mechanical Engineering, vol.11, No.11, https://doi.org/10.1177/1687814019880987.

[6] Ali F., Arif M., Khan I., Sheikh N.A. and Saqib M. (2018): *Natural convection in polyethylene glycol-based molybdenum disulfide nanofluid with thermal radiation, chemical reaction and ramped wall temperature*.– Int. J. Heat Technology, vol.36, No.2, pp.619-631, https://doi.org/10.18280/ijht.360227.

[7] Iqbal Z., Khan M., Shoaib M., Matoog, R.T., Muhammad T. and El-Zahar E.R. (2022): *Study of buoyancy effects in unsteady stagnation point flow of Maxwell nanofluid over a vertical stretching sheet in the presence of Joule heating*.–Waves in Random and Complex Media, pp.1-15, https://doi.org/10.1080/17455030.2022.2028932.

[8] Senthilvadivu K., Eswaramoorthi S., Loganathan K. and Abbas M. (2024): *Time-dependent Darcy Forchheimer flow of Casson hybrid nanofluid comprising the CNTs through a Riga plate with nonlinear thermal radiation and viscous dissipation*.– Nanotechnology Reviews, vol.13, No.1, pp.2023-0202, https://doi.org/10.1515/ntrev-2023-0202.

[9] Ganga U.R., Janaiah Ch., and Goud B.S. (2024): *Thermal diffusion and diffusion thermo effects on axi-symmetric boundary layer flow of nanofluid due to non-linear stretching sheet along the radial direction in presence of magnetic field*.– Int. J. Applied Mechanics and Engineering, vol.29, No.3, pp.32-46, https://doi.org/10.59441/ijame/190394.

[10] Mesbah A., Allouaoui R., Bouaziz A.M., and Bouaziz N.M. (2024): *Entropy generation analysis of MHD micropolar-nanofluid flow over a moved and permeable vertical plate*.– Int. J. Applied Mechanics and Engineering, vol.29, No.1, pp.73-89, DOI: https://doi.org/10.59441/ijame/175807.

[11] Medisetty P.D., Suripeddi S., Kuppalapalle V. and Badeti S. (2024): *Pulsatile MHD flow of two immiscible nanofluid through a porous channel with slip effects*.– Int. J. Applied Mechanics and Engineering, vol.29, No.1, pp.105-129, https://doi.org/10.59441/ijame/175745.

[12] Samad Khan A., Gul T., Muhammad T., Ali Yousif B.A. and Shaaban A.A. (2024): *Hybrid nanofluids flow over a Riga plate surrounded by a variable porous medium for heat transfer optimization*.– Numerical Heat Transfer, Part A: Applications, pp.1-15, https://doi.org/10.1080/10407782.2024.2345856.

[13] Bilal M., Maiz F., Farooq M., Ahmad H., Nasrat M.K. and Ghazwani H.A. (2025): *Novel numerical and artificial neural computing with experimental validation towards unsteady micropolar nanofluid flow across a Riga plate*.– Sci. Rep., vol.15, p.759, https://doi.org/10.1038 /s41598-024-84480-3.

[14] Tlili I., Nabwey H.A., Ashwinkumar G.P. and Sandeep. N. (2020): *3-D magnetohydrodynamic AA7072-AA7075/methanol hybrid nanofluid flow above an uneven thickness surface with slip effect*.– Scientific Reports, vol.10, No.4265, https://doi.org/10.1038/s41598-020-61215-8.

[15] El-Zahar E.R., Rashad A.M., Saad W. and Seddek L.F. (2020): *Magneto-hybrid nanofluids flow via mixed convection past a radiative circular cylinder.*– Scientific Reports, vol.10, p.10494, https://doi.org/10.1038/s41598-020-66918-6.

[16] Alarabi T., Rashad A.M. and Mahdy A. (2021): *Homogeneous–heterogeneous chemical reactions of radiation hybrid nanofluid flow on a cylinder with Joule heating: nanoparticles shape impact.*– Coatings, vol.11, p.1490, https://doi.org/10.3390/ coatings1112149.

[17] Mahdy A., Rashad A.M., Saad W. and Al-Juaydi H. (2021): *The magneto-natural convection flow of a micropolar hybrid nanofluid over a vertical plate saturated in a porous medium*.– Fluids, vol.6, p.202, https:// doi.org/10.3390/fluids606020.

[18] El-Zahar E.R., Mahdy A.E.N., Rashad A.M., Saad W., and Seddek L.F. (2021): *Unsteady MHD mixed convection flow of non-Newtonian Casson hybrid nanofluid in the stagnation zone of sphere spinning impulsively*.– Fluids, vol.6, No.6, pp.197, https://doi.org/10.3390/fluids6060197.

[19] Hossam A.N., Rashad A.M. and Waqar K. (2021): *Slip microrotation flow of silver-sodium alginate nanofluid via mixed convection in a porous medium*.– Mathematics, vol.9, pp.3232, https://doi.org/10.3390/math9243232.

[20] Zhang L., Bhatti M.M, Michaelides E.E., Marin M. and Ellahi R. (2022): *Hybrid nanofluid flow towards an elastic surface with tantalum and nickel nanoparticles, under the influence of an induced magnetic field*.– The European Physical Journal Special Topics, vol.231, No.3, pp.521-533, https://doi.org/10.1140/epjs/s11734-021-00409-1.

[21] Lone S.A., Alyami M.A., Saeed A., Dawar A., Kumam P. and Kumam W. (2022): *MHD micropolar hybrid nanofluid flow over a flat surface subject to mixed convection and thermal radiation.*– Scientific Reports, vol.12, No.17283, https://doi.org/10.1038/s41598-022-21255-8.

[22] Rekha M.B., Sarris I.E., Madhukesh J.K., Raghunatha K.R. and Prasannakumara B.C. (2022): *Activation energy impact on flow of AA7072-AA7075/water-based hybrid nanofluid through a cone, wedge, and plate*.– Micromachines, vol.13, No.2, pp.302, https://doi.org/10.3390/mi13020302.

[23] Verma L., Meher R., Hammouch Z. and Baskonus H.M. (2022): *Effect of heat transfer on hybrid nanofluid flow in converging/diverging channel using fuzzy volume fraction*.-Scientific Reports, vol.12, No.20845, https://doi.org/10.1038/s41598-022-24259-6.

[24] Jaafar A., Waini I., Jamaludin A., Nazar R. and Pop I. (2022): *MHD flow and heat transfer of a hybrid nanofluid past a nonlinear surface stretching/shrinking with effects of thermal radiation and suction*.– Chinese Journal of Physics, vol.79, pp.13-27, https://doi.org/10.1016/j.cjph.2022.06.026.

[25] Ullah H. Abas S.A., Fiza M., Khan I., Rahimzai A.A. and Akgul A. (2024): *A numerical study of heat and mass transfer characteristic of three-dimensional thermally radiated bi-directional slip flow over a permeable stretching surface*.– Scientific Reports, vol.14, No.19842, https://doi.org/10.1038/s41598-024-70167-2.

[26] Rao S. and Deka P.N. (2024): *Numerical analysis of MHD hybrid nanofluid flow over a porous stretching sheet with thermalradiation*.– Int. J. Appl. Comput. Math., vol.10, No.95, https://doi.org/10.1007/s40819-024-01734-4.

[27] Verma L. and Meher R. (2024): *Study on MHD hybrid nanofluid flow with heat transfer in a stretchable converging/diverging channel embedded in a porous medium with uncertain volume fraction*.– Numerical Heat Transfer, Part B: Fundamentals, pp.1-32, https://doi.org/10.1080/10407790.2024.2357617.

[28] Imoro I., Etwire C.J. and Musah R. (2024): *MHD flow of blood-based hybrid nanofluid through a stenosed artery with thermal radiation effect*.– Case Studies in Thermal Engineering, vol.59, No.104418, https://doi.org/10.1016/j.csite.2024.104418.

[29] Naik R.N., Suneetha S., Babu K.S.S. and Babu M.J. (2024): *Entropy optimization in ternary hybrid nanofluid flow over a convectively heated bidirectional stretching sheet with Lorentz forces and viscous dissipation: a Cattaneo–*

Christov heat flux model.– Proceedings of the Institution of Mechanical Engineers, Part E: J. Process Mechanical Engineering, https://doi.org/10.1177/09544089241275779.

[30] Tao H., Aldlemy M.S., Homod R.Z., Aksoy M., Mohammed M.K.A., Alawi O.A., Togun, H., Goliatt L., Khan M.M.H. and Yaseen Z.M. (2024): *Hybrid nanocomposites impact on heat transfer efficiency and pressure drop in turbulent flow systems: application of numerical and machine learning insights*.– Scientific Reports, vol.14, No.19882, https://doi.org/10.1038/s41598-024-69648-1.

[31] Maiti H., Mukhopadhyay S. and Vajravelu K., (2024): *Hybrid nanofluid flow over an unsteady stretching/shrinking disk with thermal radiation*.– Int. J. Modern Physics B, vol.38, No.7, pp.2450220, https://doi.org/10.1142/S0217979224502205.

[32] Ansari M.S., Magagula V.M. and Trivedi M. (2020): *Jeffrey nanofluid flow near a Riga plate: spectral quasilinearization approach*.– Heat Transfer, vol.49, No.3, pp.1491-1510, https://doi.org/10.1002/htj.21673.

[33] Prabakaran R., Eswaramoorthi S., Loganathan K. and Gyeltshen S. (2022): *Thermal radiation and viscous dissipation impacts of water and kerosene-based carbon nanotubes over a heated Riga sheet*.– Journal of Nanomaterials, vol.2022, Article ID 1865763, https://doi.org/10.1155/2022/1865763.

[34] Wahid N.S., Arifin N.M., Khashi'ie N.S., Pop I., Bachok N. and Hafidzuddin M.E.H. (2022): *Hybrid nanofluid stagnation point flow past a slip shrinking Riga plate*.– Chinese Journal of Physics, vol.78, pp.180-193, https://doi.org/10.1016/j.cjph.2022.05.016.

[35] Ali A., Ahmed M., Ahmad A. and Nawaz R. (2023): *Enhanced heat transfer analysis of hybrid nanofluid over a Riga plate: Incorporating Lorentz forces and entropy generation*.– Tribology International, vol.188, No.108844, https://doi.org/10.1016/j.triboint.2023.108844.

[36] Algehyne E.A., Lone S.A., Raizah Z., Eldin S.M., Saeed A. and Galal M. (2023): *Chemically reactive hybrid nanofluid flow past a Riga plate with nonlinear thermal radiation and a variable heat source/sink*.– Frontiers in Materials, vol.10, p.1132468, https://doi.org/10.3389/fmats.2023.1132468.

[37] Yasmin H., Hejazi H.A., Lone S.A., Raizah Z. and Saeed A. (2023): *Time-independent three- dimensional flow of a water-based hybrid nanofluid past a Riga plate with slips and convective conditions: a homotopic solution*.– Nanotechnology Reviews, vol.12, No.1, pp.20230183, https://doi.org/10.1515/ntrev-2023-0183.

[38] Siddique I., Khan Y., Nadeem M., Awrejcewicz J. and Bilal M. (2023): *Significance of heat transfer for second-grade fuzzy hybrid nanofluid flow over a stretching/shrinking Riga wedge*.– AIMS Mathematics, vol.8, No.1, pp.295-316, doi: 10.3934/math.2023014.

[39] Khan A.S., Ishaq M., Awwad F.A., Ismail E.A.A. and Gul T. (2024): *Flow of Magnetohydrodynamic blood-based hybrid nanofluids with double diffusion in the presence of Riga plate for heat optimization and drug applications*.– Advances in Mechanical Engineering, vol.16, No.5, https://doi.org/10.1177/16878132241244916.

[40] Upreti H., Mishra S.R., Pandey A.K. and Pattnaik P.K. (2024): *Thermodynamics analysis of Casson hybrid nanofluid flow over a porous Riga plate with slip effect*.– Int. J. Multiphysics and Multiscale Computing Engineering, vol.22, No.5, pp.19-34, doi: 10.1615/IntJMultComp Eng.2023043190.

[41] Royand N.C. and Pop I. (2021): *Exact solutions of Stokes' second problem for hybrid nanofluid flow with heat transfer*.– Physics of Fluids, vol.33, No.6, p.063603, https://doi.org/10.1063 /5.0054576.

[42] Saqib M., Khan I. and Shafie S. (2019): *Application of fractional differential equations to heat transfer in hybrid nanofluid: modelling and solution via integral transforms*.– Advances in Differential Equations, vol.2019, No.52, https://doi.org/10.1186/s13662-019-1988-5.

[43] Zulkiflee F., Shafie S. and Mohamad A.Q. (2020): *Unsteady free convection flow of nanofluids between vertical oscillating plates with mass diffusion*.– J. Advanced Research in Fluid Mechanics and Thermal Sciences, vol.76, No.2, pp.118-131.

Received: December 23, 2024
Revised: April 7, 2025